Modified Nonabsorptive Chessboard Configuration for Radar Cross Section Reduction

Amir Firouzfar[1], Majid Afsahi[2]

Abstract— **This paper presents a modified nonabsorptive radar cross-section (RCS) reducer based on previous reports. The design is a flat 4×4 chessboard, followed by two upper and lower dielectrics with the same relative permittivity and thickness. The lower dielectric is metal-backed. The incident wave to the surface of the upper dielectric penetrates through the structure. Some parts of the incident wave is reflected back by the black (metal) sections of the chessboard in the middle, while the remaining parts of the wave penetrates further in the lower dielectric until it is totally reflected by the ground plane. The relative permittivity and dielectric thicknesses are computed analytically to make a 180° phase difference between the two reflected waves. This results in destructive interference and makes a null in the expected angle of reflection. The theory of operation is deduced generally for any angle of incidence as well as both principal polarizations. First, the designing procedure is done with MATLAB, then the practical design is simulated with Ansys HFSS13 and finally, it is fabricated and its monostatic RCS reduction property is measured experimentally. At least 10dB RCS reduction compared to a metal plate of the same size is guaranteed from 8.5 to 17.5 GHz for normal incidence.**

Index Terms — **radar cross section (RCS) reduction, chessboard, nonabsorptive.**

I. INTRODUCTION

S The level of the back scattered electromagnetic power from an object and reducing it, when the object is illuminated by an incident field is an important parameter especially for military applications. The quantity which explains the scattering property of the object is its radar cross section (RCS) [1-5]. There are a variety of methods proposed in the literature to reduce RCS. Generally, one of these methods is shaping the object [6, 7], or redirecting the incoming waves away from the radar receiver. Using planar RCS reducers are easier in many cases [8-11]. One can divide planar RCS reducers in two distinct categories: 1- absorptive structures; 2- nonabsorptive structures. In absorptive structures the electromagnetic energy is converted to heat the structure [2]. Salisbury screen is a well-known structure to reduce the RCS which suffers from being bulky or narrow

band [12]. Loading absorbing dielectrics with a proper frequency selective surface (FSS) [13-16] and/or perforating it, is another way of improving the absorbing properties of the dielectric [17-19]. The problems with these designs are the cast, scarcity of such dielectrics and manufacturing difficulties. Perforating a dielectric in a periodic manner with acceptable accuracy is a hard task. Another way of designing planar absorbers is to load a lossless dielectric with some lossy FSS. An example of such designs acting in W band is presented in [20]. Although the practical return loss response of the absorber presented in [20] is very good, hardness of fabrication is its main deficiency. The procedure for designing such an absorber can be explained simply as follows (transmission line model): The structure is a lossy FSS, mounted on a metal-backed dielectric. The zero impedance of the ground plane will be transferred to the surface of the dielectric, where it will be paralleled with the impedance of the FSS. The total impedance must be matched to the free space impedance. To make the design feasible, it is needed to make the real part of the FSS impedance, high to some extent. To reach this goal, usually it is necessary to fabricate some especial metal or alloy with a very small dielectric thickness which needs modern technology. In [20], two designs are presented: (a) An array of 20×20 Nichrome circles on a 0.5 mm thick PMMA substrate, where the circle thickness is 15 nm, (b) An array of 40×40 Nichrome rings on a 0.25 mm thick Alumina substrate. The ring thickness is 30 nm. As an introduction to a more update reference, using the so-called method, we can refer to [21], in which resistive treble-square loops are exploited. In [21] only the simulation results are presented. Furthermore, the recommended material used for the FSS layer is tantalum nitride which cannot be found easily. In [22] a procedure is presented in order to select the resistance for broadband absorption based on lossy FSS printed on a lossless, metal-backed dielectric. Polarization rotation or conversion is another way to reduce RCS [23, 24].

Another practical method to reduce RCS is to use lossless flat structures [5, 16]. The main advantages of these structures are low profiles and ease of fabrication using printed circuit technology. The theory behind this method is to distribute the incoming waves away from the expected direction of reflection. Using chessboard configuration is a common procedure to make a 180º phase difference between the reflected waves from the black and white sections of the chessboard [16]. In [25] and [26], PEC (Perfect Electric

---

1: A. Firouzfar, is with TIC (Ministry of ICT, Telecommunication Infrastructure Company, Tehran, Iran), Email: a.firouzfar@tic.ir

2: M. Afsahi, is with the Electrical Engineering Department, Semnan University, Semnan, Iran. Email: m_afsahi@semnan.ac.ir.

Conductor) and AMC (Artificial Magnetic Conductor [27]) structures are used as black and white sections of the chessboard. Unfortunately, AMC structures cannot be realized at a very large bandwidth, therefore the recommended structure in [25] is narrowband. This problem has been resolved in [28] by replacing the PEC with another AMC but with a different resonant frequency. In [29] a novel design is introduced by comparing a periodic chessboard design with an aperiodic one. It is shown that the aperiodic structure can have a much better performance than the periodic one. It is claimed by the authors that no attempt has been done in order to optimize the final design. Further efforts for optimization may result in a better response.

A simple chessboard configuration for RCS reduction is presented in [30]. Here a modified configuration with a different theory is presented by adding a superstrate which results in a better performance in terms of bandwidth and angular stability. The design presented here is based on the phase difference between two portions of waves reflected back from two sets of metal-backed dielectrics. The relative permittivity and thickness of dielectrics are designed to produce a 180º phase difference in the desired frequency. In order to make the design flat, a 4×4 chessboard is fabricated on top of a metal-backed dielectric. Another dielectric is pressed on the top of the chessboard as a superstrate. The black (metal) parts of the chessboard act as ground for some parts of the incoming wave while the remaining part of the energy is reflected back by the ground plane in the bottom.

This paper has been structured as follows. In Section II, the theoretical procedure for designing two sets of dielectrics (with the same relative permittivities and different thicknesses) is presented. The proposed design method is associated with oblique incidence with both principal polarizations (TE and TM). Section III focuses on the practical simulations and measurement in laboratory to finalize with conclusions in Section IV..

II. PRINCIPLE OF OPERATION

To construct a mathematical basis for the design, an infinite dimension metal-backed dielectric plate illuminated by an incident wave with an arbitrary wavelength can be considered (Figure 1). Two different polarizations (TE and TM with respect to direction of incidence) are considered.
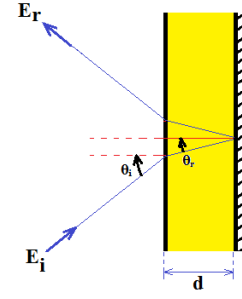

Figure 1: Diagram of a metal-backed dielectric, illuminated by an incident wave

One can define TE and TM impedances for a wave traveling with angle " θ " with respect to an assumed axis as follows:

$$Z_{TM}^{media} = Z_0^{media} \cos(\theta), \quad Z_{TE}^{media} = Z_0^{media} / \cos(\theta). \tag{1}$$

For the configuration of Figure 1, the incident wave travels with angle " θ_i " while the transmitted wave to the dielectric propagates with angle " θ_r ", which can be found using Snell's law:

$$\theta_r = \sin^{-1}(\sin(\theta_i)/\sqrt{\varepsilon_r}). \tag{2}$$

In (2), it is assumed that the dielectric is non-magnetic and its relative permittivity is " ε_r ". The zero impedance of the ground can be transferred to the surface of the dielectric by the following formula:

$$Z_{TE,TM}^{Trans} = jZ_{TE,TM}^{dielectric} \tan[k_d d \cos(\theta_r)]. \tag{3}$$

where, " k_d " is the wavenumber in the dielectric. The reflection coefficient from the surface of the dielectric is calculated as follows:

$$\Gamma_{TM,TE} = \frac{Z_{TM,TE}^{trans} - Z_{TM,TE}^{air}}{Z_{TM,TE}^{trans} + Z_{TM,TE}^{air}}. \tag{4}$$

Now, the two dielectrics with different thicknesses (d_1 and d_2) can be considered to a have 180º phase difference. Non-absorptive dielectrics are assumed, so this leads to:

$$\Gamma_{TM,TE}^{(1)} = -\Gamma_{TM,TE}^{(2)}$$
$$\Rightarrow \frac{Z_{TM,TE}^{trans1} - Z_{TM,TE}^{air}}{Z_{TM,TE}^{trans1} + Z_{TM,TE}^{air}} = -\frac{Z_{TM,TE}^{trans2} - Z_{TM,TE}^{air}}{Z_{TM,TE}^{trans2} + Z_{TM,TE}^{air}}$$
$$\Rightarrow Z_{TM,TE}^{trans1}.Z_{TM,TE}^{trans2} = (Z_{TM,TE}^{air})^2. \tag{5}$$

By substituting (3) in (5) one can deduce:

$$\tan[k_d d_1 \cos(\theta_r)].\tan[k_d d_2 \cos(\theta_r)]$$

$$= -\left(\frac{Z_{TM,TE}^{air}}{Z_{TM,TE}^{dielectric}}\right)^2 = \begin{cases} -\varepsilon_r \left(\dfrac{\cos(\theta_i)}{\cos(\theta_r)}\right)^2 & TM \\[2em] -\varepsilon_r \left(\dfrac{\cos(\theta_r)}{\cos(\theta_i)}\right)^2 & TE \end{cases}$$

(6)

We can further proceed by considering the normal incidence and checking the design for the general case. By this assumption, $\theta_i = \theta_r = 0$, so (6) reduces to:

$$\tan(k_d d_1).\tan(k_d d_2) = -\varepsilon_r$$

(7)

For practical reasons, the smallest values of d_1 and d_2 are preferred. Furthermore, a dielectric with an arbitrary thickness may not be found, so we must pay attention for the feasibility of quantities "d_1" and "d_2". One way of solving (7) is to choose "d_1" and "d_2", such that:

$$\begin{cases} \tan(k_d d_1) = -\sqrt{\varepsilon_r} \\ \tan(k_d d_2) = \sqrt{\varepsilon_r} \end{cases} \Rightarrow \begin{cases} k_d d_1 = \pi - \arctan(\sqrt{\varepsilon_r}) \\ k_d d_2 = \arctan(\sqrt{\varepsilon_r}) \end{cases}$$

(8)

Given specified quantities to "ε_r", d_1 and d_2 can be found using (8). Parametric diagrams can be depicted to seek for the best "ε_r". The criteria for judging the performance of different designs are the bandwidth in which the phase difference maintains 180º ± 30º, as well as feasibility of dielectrics with the specified thicknesses. Figure 2 is one of such parametric diagrams for normal incidence. As can be seen, $\varepsilon_r = 3$ has the widest bandwidth. The relative permittivity of Rogers\RO3003 is 3 and it is ideal for this design. Unfortunately, we could not find RO3003, so we used RO4003B whose relative permittivity is 3.55. Indeed the ideal performance will be deteriorated due to this substitution, as is shown in Figure 2. The next figures (Figure 3 and Figure 4) depict the destructive interference of waves for oblique incidence for the computed thicknesses (d_1 and d_2 previously).
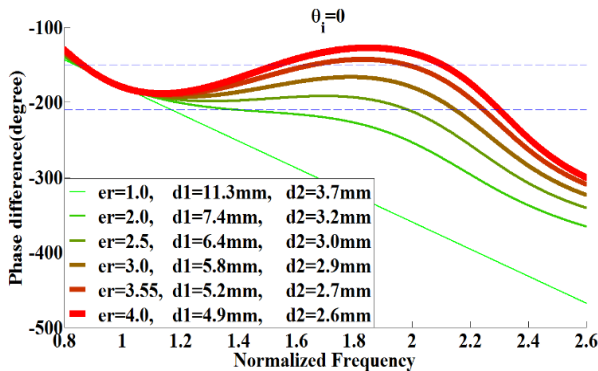

Figure 2: Parametric diagram of phase difference between the reflection coefficients of different thickness, metal-backed dielectrics designed to have 180º phase difference in $f = f_0$ for normal incidence. The diagram is for normal incidence.

As can be seen from Figures 2-4, the designs show a better performance in frequencies greater than the design frequency. In order to have a true conclusion, "f_{ave}" is introduced as the average frequency in which the phase difference is maintained in the region of 180º ± 30º. We have summarized the design performances in Table I in terms of normalized bandwidth ($bw = \Delta f/f_{ave}$) for normal incidence, oblique incidence stability ($\Delta \varphi$ = Maximum oblique incidence angle in which the phasecancelation remains in the range of 180º ± 30º from $0.9f_{ave}$ to $1.1f_{ave}$ for both principal polarizations), and the dielectric thicknesses in terms of the free-space wavelength in f_{ave}. As is obvious from Table I, $\varepsilon_r = 3$ has the best bandwidth for normal incidence.
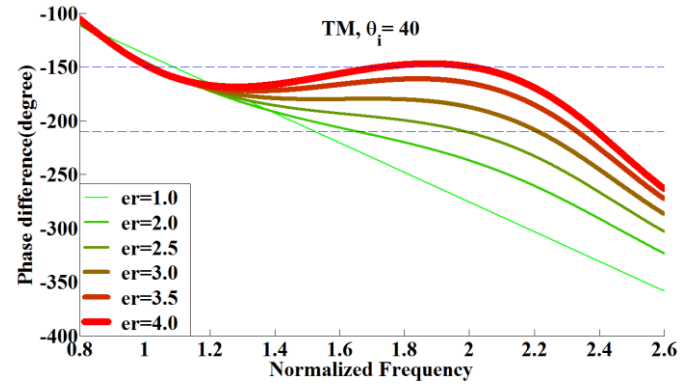

Figure 3: Parametric diagram of phase difference between the reflection coefficients of different thickness, metal-backed dielectrics designed to have 180º phase difference in $f = f_0$ for normal incidence. The diagram is for oblique incidence of $\theta_i = 40º$ for TM polarization.
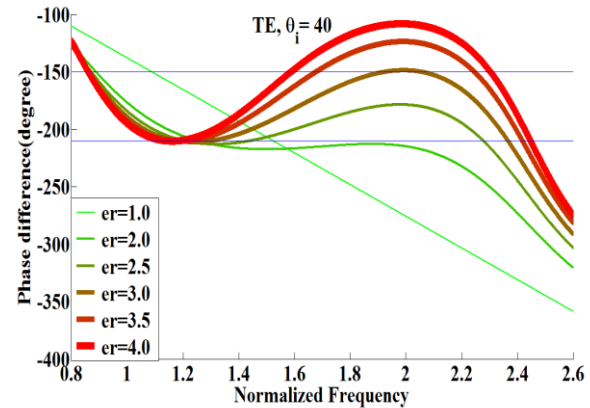

Figure 4: Parametric diagram of phase difference between the reflection coefficients of different thickness, metal-backed dielectrics designed to have 180º phase difference in $f = f_0$ for normal incidence. The diagram is for oblique incidence of $\theta_i = 40º$ for TE polarization.

TABLE 1: COMPARISON OF PERFORMANCE IN TERMS OF BANDWIDTH AND ANGULAR STABILITY AND DIELECTRIC THICKNESSES FOR DIFFERENT DESIGNS.

ε_r	$\Delta f/f_{ave}$	$\Delta \varphi$	d_1/λ_{ave}	d_2/λ_{ave}
1	0.33	23º	0.38	0.12

.00				
2.00	0.48	37°	0.27	0.12
2.50	0.80	36°	0.30	0.14
3.00	0.86	39°	0.29	0.14
3.55	0.64	47°	0.22	0.11
4.00	0.56	46°	0.20	0.10

III.   SIMULATION AND MEASUREMENT

All the statements mentioned before are purely theoretical, because the metal-backed dielectrics are assumed to have infinite dimensions. In order to realize a practical RCS reducer, first some simulations are carried out and the best of them is fabricated and measured in the laboratory. In order to dedicate a quantity to measure the figure of merit for bi-static RCS reduction, "FMB" is defined following [29].

$$FMB(f) = \frac{Max\{Bistatic \; RCS \; with \; RCS \; reducer\}}{Max\{Bistatic \; RCS \; without \; RCS \; reducer\}}$$

Where the Max function domain covers all bi-static scattering angles (θ_s, φ_s) ($0 \le \theta_s \le 90°$ and $0 \le \varphi_s \le 360°$) for a given frequency f and incident angle (θ_i, φ_i).

A standard 30.38×45.72 cm (12×18 in) sheet with 0.8mm (32 mil) thickness is cut to make 6 congruent squares. The dimensions of each square are 15.24×15.24 cm (6×6 in). A 4×4 chessboard is fabricated on one side of one of these squares when the other copper layer is removed. Here each chessboard square has a 3.81×3.81cm dimension, which is about the maximum wavelength in the design frequency (8.5-17GHz). This is to approximate infinite ground for each black chessboard square. If we choose less size for each square, it may not act as infinite ground for the maximum wavelength in the band (3.5 cm for 8.5GHz). The copper on each side of the remaining squares is removed except one layer of one of them to be used as the ground plane. The 6 squares are stuck above each other precisely to construct the final design (15.24×15.24 cm with 6×0.8 mm = 4.8mm thickness). The ground plane is the lower layer and the chessboard is in the middle. Finally, two sets of metal-backed dielectrics are realized in a planar structure. One set is from the surface of the design to the black (copper) sections of the chessboard in the middle ($d_2 = 3 \times 0.8$ mm = 2.4mm), while the other set is from the surface to the ground plane through white sections of the chessboard ($d_1 = 6 \times 0.8$ mm = 4.8 mm). The fabricated chessboard (before sticking the upper layers) is depicted in Figure 5. Before fabrication and measurement, the whole structure was simulated in AnsysHFSS13. The numerical results obtained from Ansys HFSS13 are exported to MATLAB in order to calculate FMB.

The FMB parameters are depicted in Figure 6 for different angles of incidence. One can compare the performance of design with $\varepsilon_r=3$.

The incident wave to the surface of the structure will be distributed to other directions. The monostatic RCS is a measure of the reflected wave from the specular angle (the radar transmitter and receiver are coincide) but the FMB is a measure of reflected wave to all directions. Therefore, it reveals the RCS reducer performance better than monostatic RCS. For example, maybe some designs have a very good phase cancellation in some directions, but the FMB is not ideal. In fact, in such cases the design will properly force the incoming wave away from the expected angle of reflection, but it peaks in another direction. A more uniform distribution
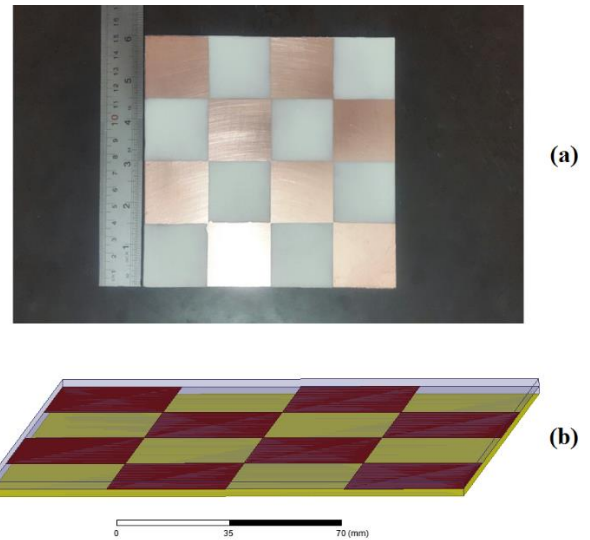

Figure 5: (a) The constructed 15.24×15.24 cm chessboard layer of ROGERS/RO4003 before sticking the upper dielectric layers, (b) 3D view of the design with the superstrate.
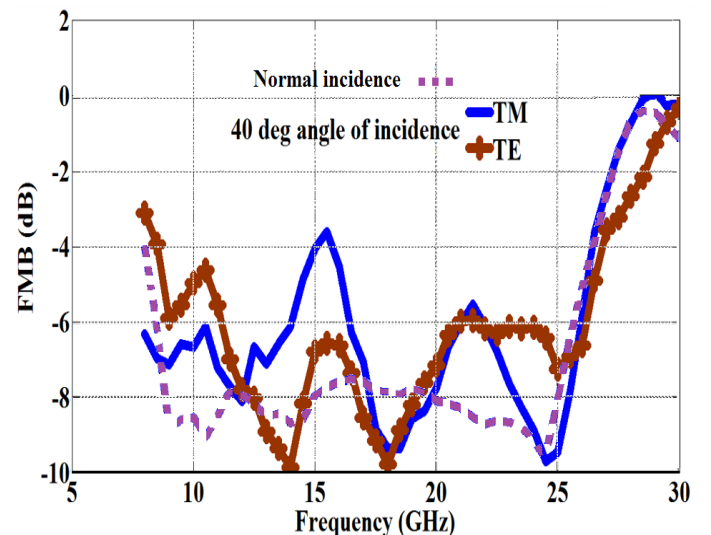

Figure 6: FMB parameters for normal incidence, and 40° of

incidence for $\varepsilon_r = 3.55$.

of electromagnetic power by the RCS reducer is better. In Figure 7, the 3D view of distributing the incoming wave by the design is compared to that of a flat PEC sheet with the same dimensions for $f = 15$GHz.

To validate the predicted performance of the design, monostatic RCS was measured from 8 to 18GHz in antenna laboratory of University of Tehran. Due to difficulties with bi-static RCS measurement, we could not calculate the FMB parameter. Figure 8 is a picture of test setup. Two identical horn antennas were placed near each other and were connected to PNA Vector Network Analyzer (E8361C), while the DUT was in the far field of them.

Figure 8: Test set up diagram for monostatic RCS measurement

In Figure 9, we can compare the results of simulation with measurement for monostatic RCS reduction. At least a 10dB RCS reduction is guaranteed from 8.5 to 17.5GHz based on the practical measurement. The difference between the two diagrams maybe due to imperfect manufacturing of DUT, imperfect antenna setup or pyramidal absorbers in testing room.
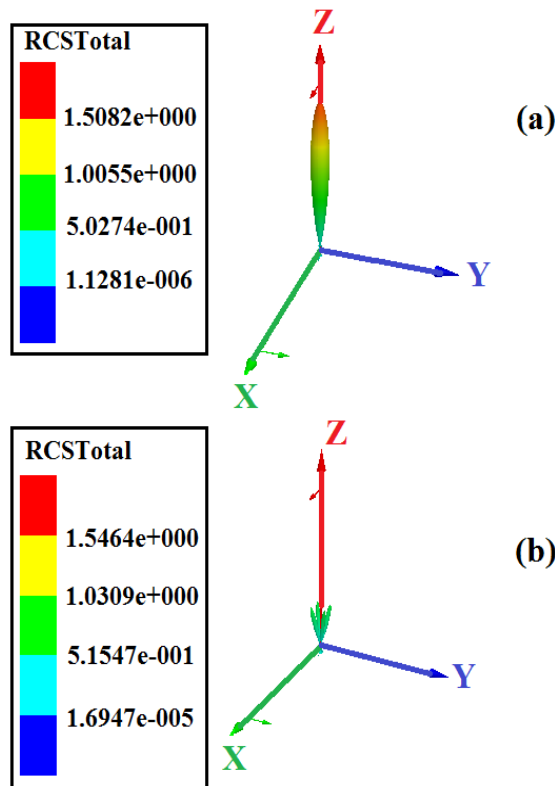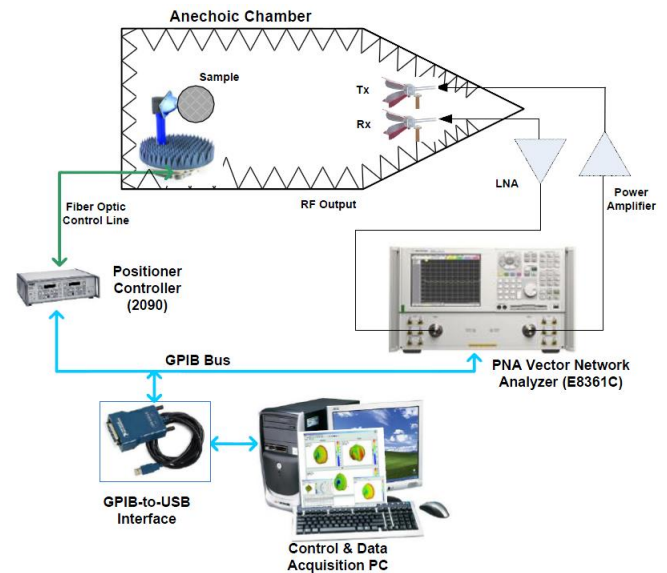

Figure 7: Depiction of the ability of the design to distribute the incident wave away from the specular direction in 15 GHz. (a) A flat PEC sheet with the same size as the proposed design, (b) The simulation is done by Ansys HFSS11.
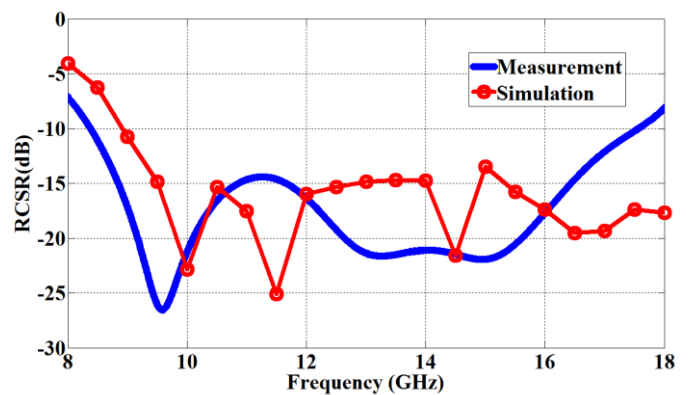

Figure 9: Comparison of RCS reduction between simulation and measurement. Two distinct tests were carried out as well as two simulations: one for the proposed design; the other for a metallic plate with the same size.

To compare the performance of this work with a recently reported paper [29], Table II is presented for various aspects of merit.

TABLE 2: COMPARISON OF PERFORMANCE BETWEEN PRESENT STUDY AND [29]

Figure of merit	Present study	[29]
Simulated bandwidth for FMB <6dB	8-27GHz (108.5%)	8.5-18GHz (71.7%)
Thickness/λ	0.13	0.09

max		
Dimensions/ λ_{max}	4.0×4.0	4.7×4.7
Ease of fabrication	Easy to fabricate (only one layer fabrication is needed),	Difficult to fabricate (2 layers fabrication),
Prise	Cheap, because of using RO4003.	Expencive, because of using RT/duroid 5880.

IV. CONCLUSION

A new method for reducing radar cross section is presented. This method is based on phase cancellation of reflected waves from two sets of metal-backed dielectrics with different thicknesses. We devised a method to realize this idea in a completely flat design. The chessboard configuration for reducing RCS is reported in many papers, but the novelty of this work is to use a completely different method to realize the aim which is based on different thicknesses of dielectrics.

The mathematical relations to realize this idea is introduced. The proposed theory is general so it contains all incident angles and two principal polarizations. We have assumed dielectrics with equal relative permittivities. Given a quantity to "ε_r", there will be a unique set of dielectric thicknesses (d_1 and d_2) based on the presented recommendation. Therefore, there will remain a single quantity (ε_r) to be optimized to have RCS reduction in a wide frequency band and angular and polarization stability. The feasibility of dielectric thicknesses must be considered. We figured out that ε_r= 3, can produce the best bandwidth but we could not find a dielectric with such ε_r. Before manufacturing, the simulations were carried out using Ansys HFSS13. Finally, an instant of such designs is produced using ROGERS\RO4003B. The result of the RCS reduction shows a tendency to deteriorate for higher frequencies, where the simulation is good. It may be due to insufficient accuracy of fabrication and overall thickness of the six layers above each other.

V. REFERENCES

[1] G. T. Ruck, D. E. Barrick, W. D. Stuart, and C. K. Krichbaum, *Radar Cross Section Handbook. Volumes 1 & 2*: Plenum Press, New York, 1970.

[2] C. Chen, Z. Li, L. L. Liu, J. Xu, P. Ning, B. Xu, *et al.*, "A circularly-polarized metasurfaced dipole antenna with wide axial-ratio beamwidth and RCS reduction functions," *Progress In Electromagnetics Research,* vol. 154, pp. 79-85, 2015.

[3] J. Zhang, J. Xu, Y. Qu, J. Ding, and C. Guo, "A microstrip antenna with reduced in-band and out-of-band radar cross-section," *International Journal of Microwave and Wireless Technologies,* pp. 1-7.

[4] J. Zhang, H. Li, Q. Zheng, J. Ding, and C. Guo, "Wideband radar cross-section reduction of a microstrip antenna using slots," *International Journal of Microwave and Wireless Technologies,* vol. 10, pp. 1042-1047, 2018.

[5] A. Ghayekhloo, M. Afsahi, and A. A. Orouji, "An optimized checkerboard structure for cross-section reduction: Producing a coating surface for bistatic radar using the equivalent electric circuit model," *IEEE Antennas and Propagation Magazine,* pp. 1-1, 2018.

[6] F. Costa, S. Genovesi, and A. Monorchio, "A frequency selective absorbing ground plane for low-RCS microstrip antenna arrays," *Progress In Electromagnetics Research,* vol. 126, pp. 317-332, 2012.

[7] X. Zhu, W. Shao, J.-L. Li, and Y.-L. Dong, "Design and optimization of low RCS patch antennas based on a genetic algorithm," *Progress In Electromagnetics Research,* vol. 122, pp. 327-339, 2012.

[8] M. Shabani and A. Mir, "Design and Analysis of an Ultra-Broadband Polarization-Independent Wide-Angle Plasmonic THz Absorber," *IEEE Journal of Quantum Electronics,* vol. 57, pp. 1-8, 2021.

[9] B. Noorbakhsh, A. Abdolali, and M. Janforooz, "In-band radar cross-section reduction of the slot array antennas by RAM-based frequency selective surfaces," *IET Microwaves, Antennas & Propagation,* 2021.

[10] G. Gonçalves Machado, R. Cahill, V. Fusco, and G. Conway, "Frequency selective superstrate absorber for wideband RCS reduction of metal-backed antennas," *IET Microwaves, Antennas & Propagation,* 2021.

[11] F. He, K. Si, D. Zha, R. Li, Y. Zhang, J. Dong, *et al.*, "Broadband Microwave Absorption Properties of a Frequency-Selective Surface Embedded in a Patterned Honeycomb Absorber," *IEEE Transactions on Electromagnetic Compatibility,* 2021.

[12] R. L. Fante and M. T. Mccormack, "Reflection properties of the Salisbury screen," *IEEE transactions on antennas and propagation,* vol. 36, pp. 1443-1454, 1988.

[13] L. Alonso-González, S. Ver-Hoeye, M. Fernandez-Garcia, and F. Las Heras Andres, "Layer-to-Layer Angle Interlock 3D Woven Bandstop Frequency Selective Surface," *Progress In Electromagnetics Research,* vol. 162, pp. 81-94, 2018.

[14] A. Firouzfar, M. Afsahi, and A. A. Orouji, "Novel synthesis formulas to design square patch frequency selective surface absorber based on equivalent circuit model," *International Journal of RF and Microwave Computer-Aided Engineering,* vol. 29, p. e21680, 2019.

[15] A. Firouzfar, M. Afsahi, and A. A. Orouji, "Novel, Straightforward Procedure to Design Square Loop Frequency Selective Surfaces Based on Equivalent Circuit Model," *AEU-International Journal of Electronics and Communications,* p. 153164, 2020.

[16] A. Ghayekhloo, M. Afsahi, and A. A. Orouji, "Checkerboard plasma electromagnetic surface for wideband and wide-angle bistatic radar cross section reduction," *IEEE Transactions on Plasma Science,* vol. 45, pp. 603-609, 2017.

[17] A. Fallahi, A. Yahaghi, H.-R. Benedickter, H. Abiri, M. Shahabadi, and C. Hafner, "Thin wideband radar absorbers," *IEEE Transactions on Antennas and Propagation,* vol. 58, pp. 4051-4058, 2010.

[18] M. Bozzi and L. Perregrini, "Analysis of multilayered printed frequency selective surfaces by the MoM/BI-RME method," *IEEE Transactions on Antennas and Propagation,* vol. 51, pp. 2830-2836, 2003.

[19] F. Wang, W. Jiang, T. Hong, H. Xue, S. Gong, and Y. Zhang, "Radar cross section reduction of wideband antenna with a novel wideband radar absorbing materials," *IET*

Microwaves, Antennas & Propagation, vol. 8, pp. 491-497, 2014.

[20] F. Sakran, Y. Neve-Oz, A. Ron, M. Golosovsky, D. Davidov, and A. Frenkel, "Absorbing frequency-selective-surface for the mm-wave range," *IEEE Transactions on Antennas and Propagation,* vol. 56, pp. 2649-2655, 2008.

[21] M. Li, S. Xiao, Y.-Y. Bai, and B.-Z. Wang, "An ultrathin and broadband radar absorber using resistive FSS," *IEEE Antennas and Wireless Propagation Letters,* vol. 11, pp. 748-751, 2012.

[22] H.-B. Zhang, P.-H. Zhou, H.-P. Lu, Y.-Q. Xu, D.-F. Liang, and L.-J. Deng, "Resistance selection of high impedance surface absorbers for perfect and broadband absorption," *IEEE Trans. Antennas Propag,* vol. 61, pp. 976-979, 2013.

[23] Y. Jia, Y. Liu, Y. J. Guo, K. Li, and S.-X. Gong, "Broadband polarization rotation reflective surfaces and their applications to RCS reduction," *IEEE Transactions on Antennas and Propagation,* vol. 64, pp. 179-188, 2016.

[24] Q. Zheng, C. Guo, H. Li, and J. Ding, "Broadband radar cross-section reduction using polarization conversion metasurface," *International Journal of Microwave and Wireless Technologies,* vol. 10, pp. 197-206, 2018.

[25] M. Paquay, J.-C. Iriarte, I. Ederra, R. Gonzalo, and P. de Maagt, "Thin AMC structure for radar cross-section reduction," *IEEE Transactions on Antennas and Propagation,* vol. 55, pp. 3630-3638, 2007.

[26] S. Esmaeli and S. Sedighy, "Wideband radar cross-section reduction by AMC," *Electronics Letters,* vol. 52, pp. 70-71, 2015.

[27] L. Zhao, D. Yang, H. Tian, Y. Ji, and K. Xu, "A pole and AMC point matching method for the synthesis of HSF-UC-EBG structure with simultaneous AMC and EBG properties," *Progress In Electromagnetics Research,* vol. 133, pp. 137-157, 2013.

[28] J. C. I. Galarregui, A. T. Pereda, J. L. M. De Falcon, I. Ederra, R. Gonzalo, and P. de Maagt, "Broadband radar cross-section reduction using AMC technology," *IEEE Transactions on Antennas and Propagation,* vol. 61, pp. 6136-6143, 2013.

[29] A. Edalati and K. Sarabandi, "Wideband, wide angle, polarization independent RCS reduction using nonabsorptive miniaturized-element frequency selective surfaces," *IEEE transactions on antennas and propagation,* vol. 62, pp. 747-754, 2014.

[30] S. Simms and V. Fusco, "Chessboard reflector for RCS reduction," *Electronics Letters,* vol. 44, pp. 316-318, 2008.